Pebble bed packing in square cavities

J. Reimann
A. Abou-Sena
R. Nippen
C. Ferrero

KIT Scientific Publishing

J. Reimann, A. Abou-Sena, R. Nippen, C. Ferrero

Pebble bed packing in square cavities

Pebble bed packing in square cavities

by
J. Reimann
A. Abou-Sena
R. Nippen
C. Ferrero

KIT Scientific Publishing

Report-Nr. KIT-SR 7631

Autoren

J. Reimann, A. Abou-Sena (KIT)
R. Nippen (KBHF GmbH, Eggenstein-Leopoldshafen)
C. Ferrero (UEuropean Synchrotron Radiation Facility, Grenoble Cedex, France)

Abstract

In present ceramic breeder blanket for fusion power reactors both the ceramic breeder material and beryllium are used in form of pebbles. The interconnected quasi-square containers are filled up with pebbles through small pipes. One dimension of these containers, i.e. the pebble bed height H is much smaller than the other two dimensions. By appropriate techniques the pebble beds are densified in order to obtain a homogeneous pebble distribution within the pebble bed and a high density of the total pebble bed, characterized by the so-called packing factor.

Previous packing investigations concentrated on pebble beds consisting of spherical particles in vertical, long cylindrical cavities with a piston at the top. Both single-size (only one sphere diameter d) and multi-size systems (mixture of diameters) were investigated.

The aims of the present experiments are both the comparison of the packing behaviour of non-spherical beryllium pebbles with that of spherical beryllium particles used in the past, and the use of cavities dominated by flat walls. The available small amounts of the four non-spherical pebble batches dictated the sizes of the cavities; i) a cylindrical cavity (diameter D=50mm, maximum height H=65mm) with either a piston at the top in order to vary H or with a fixed top plate and filled through a small opening, and ii) closed parallelepidedal cavities of 100x100mm base and bed heights of 10 or 20mm, filled through a small opening. In order to broaden the experimental parameter range, further experiments were performed using single- and multi-size spherical glass, steel, and lithium orthosilicate (OSi) particles.

In pebble beds, two different zones exist: i) the bulk zone where pebbles do not show a regular arrangement, and ii) the wall zones with structured packs depending on the wall curvature. Previous tomography investigations at the European Synchrotron Radiation Facility (ESRF), Grenoble, France, revealed already many details (void distributions, contact numbers, etc.). Further analyses of these experiments were performed and local packing factors were determined for the bulk, cylindrical and flat wall zones. The important result is that the packing factors close to a flat wall are about the same as that of the bulk, whereas in the cylindrical wall zone and, even more pronounced, in corners, the packing fraction can be significantly smaller.

For pebble bed densification after filling, both vibration and/or knocking were applied. The visual observation through the Plexiglas containers walls was very helpful to judge the effectiveness of the densification parameters, e.g. the role of granular convection flows in closed cavities.

Concerning single-size pebble beds, packing factors in the cylindrical container with a movable top plate agree well with previously obtained values of 62.5% and 64.5% for the reference beryllium batch, respectively, OSi pebbles. The values for the non-spherical beryllium grades are very close to that of the

reference beryllium material, except for that grade with a significantly larger pebble roughness. Generally, it can be concluded that the packing density for all investigated single-size materials does not decrease with decreasing bed height down to at least H/d≈10.

For the fixed cavity dimensions, the development of structured packs is rendered more difficult, especially for pebbles with rough surface and/or irregular shape. In the 10mm square cavity all beryllium grades show decreased packing densities, whereas for the same height in the cylindrical cavity the reference value was reached. For small, rather smooth spherical particles, e.g. OSi, no decrease was observed in the 10mm cavity.

Using multi-size systems, segregation effects are of large concern. Even if the blended material has the defined composition during the filling, segregation due to sifting generally occurs within the cavity. Densification techniques, even visually controlled, cannot undo effectively segregation. Granular convection flow can even enhance segregation. For pebble diameter ratios larger than 7, homogeneous packings can be achieved by pouring the small pebbles into the interstices of the formerly densified and fixed larger pebbles. Packing factors of more than 84% were thus obtained. At present, this special type of binary pebble beds is, at present, not considered for the EU ceramic breeder blankets because of the potential segregation effects during cyclic blanket operation. Further investigations are required in order to prove if these effects are a critical issue.

Zusammenfassung

In derzeitigen keramischen Brutblankets für Leistungs-Kernfusionsreaktoren werden sowohl für das keramische Brutmaterial als auch für Beryllium granulare Materialien verwendet. Die miteinander verbundenen nahezu quaderförmigen Behälter werden durch kleine Rohre mit Schüttgut gefüllt. Eine Dimension dieser Behälter, nämlich die Schüttbetthöhe H, ist sehr viel kleiner als die beiden anderen Dimensionen. Durch entsprechende Techniken werden die Schüttbetten verdichtet um eine homogene Verteilung des Schüttguts im Schüttbett zu erreichen sowie eine hohe Dichte im gesamten Schüttbett, charakterisiert durch den sogenannten Schüttfaktor.

Frühere Schüttversuche konzentrierten sich auf Schüttbetten bestehend aus sphärischen Partikeln in senkrechten, langen zylindrischen Hohlräumen mit einem Kolben an der Oberseite. Sowohl Einkorn- (nur ein Korndurchmesser d) als auch Mehrkorn-Mischungen (verschiedene Durchmesser) wurden untersucht.

Das Ziel der jetzigen Experimente ist zum einen der Vergleich des Packungsverhaltens von nichtsphärischen Berylliumpartikeln mit dem von in der Vergangenheit verwendeten sphärischen Berilliumpartikeln, zum anderen die Verwendung von Hohlräumen, die durch flache Wände dominiert werden. Die kleine zur Verfügung stehende Menge der vier nichtsphärischen Beryllium-Sorten diktierte die Größen der verwendeten Hohlräume: i) Zylindrischer Hohlraum (Durchmesser 50mm, maximale Höhe H=65mm) mit entweder einem oben angeordneten Kolben um H zu variieren oder einer festen oberen Scheibe und Füllung durch eine kleine Öffnung und ii) geschlossenen quaderförmigen Hohlräumen mit Abmessungen 100x100mm und Schüttbetthöhen von 10 und 20mm, gefüllt durch eine kleine Öffnung. Um den experimentellen Parameterbereich zu erweitern wurden zudem Experimente mit Ein- und Mehrkorn-Glas- und Stahlkugeln sowie Lithium-Orthosilikat (OSi) Partikeln durchgeführt.

In Schüttbetten unterscheidet man zwei verschiedene Bereiche: i) den Kernbereich, wo die Partikel keine regelmäßige Anordnung besitzen und ii) Wandbereiche mit strukturierter Packung, abhängig von der Wandkrümmung. Frühere tomografische Untersuchungen in der European Synchrotron Radiation Facility (ESRF), Grenoble, Frankreich, zeigten bereits viele Details der Kugelanordnungen (Verteilung des Hohlvolumenanteils, Kontaktzahlen, usw.). Weitere Analysen dieser Experimente wurden durchgeführt und lokale Schüttfaktoren wurden bestimmt für den Kernbereich, zylindrische und ebene Wandbereiche. Das wichtige Ergebnis ist, dass der Schüttfaktor nahe einer ebenen Wand ungefähr den gleichen Wert besitzt wie der des Kernbereichs, während die Werte nahe zylindrischer Wände, oder noch ausgeprägter, in Eckenbereichen, sehr viel kleiner sein können.

Nach dem Einfüllen wurden die Schüttbetten durch Vibration und/oder Klopfen verdichtet. Die Beobachtung durch die Plexiglas-Wände war sehr hilfreich für die Beurteilung der Effektivität der Verdichtungsparameter, insbesondere der Bedeutung von granularen Strömungen in geschlossenen Behältern.

Die Schüttfaktoren für Einkorn-Schüttungen in dem zylindrischen Behälter mit Zylinder stimmen gut mit früheren Werten von 62,5% und 64,5% für das Referenz-Berylliummaterial, bzw. OSi überein. Die Werte für nichtsphärische Berylliumsorten stimmen recht gut mit denen des Referenzmaterials überein außer für eine Sorte mit einer deutlich größeren Rauigkeit der Partikel. Allgemein kann festgestellt werden, dass die Schüttdichte für alle untersuchten Einkorn-Systeme nicht mit fallender Schüttbetthöhe abnimmt, zumindest bis zu einem Wert H/d≈10.

Bei Hohlräumen mit festen Abmessungen wird die Ausbildung regulärer Packungen erschwert; speziell für Partikel mit rauer Oberfläche und/oder unregelmäßiger Form. Im quaderförmigen Hohlraum mit H=10mm besaßen alle Beryllium-Sorten eine niedrigere Schüttdichte, während bei gleichem H und zylindrischen Hohlräumen der Referenzwert erreicht wurde. Für kleine, glatte und nahezu sphärische Partikel, z.B. OSi, trat keine Verringerung in quaderförmigen 10mm Hohlraum auf.

Bei Mehrkorn-Mischungen sind Segregationseffekte von großer Bedeutung. Selbst wenn vorgemischtes Material mit richtiger Zusammensetzung in den Behälter eingefüllt wird, tritt im Behälter im Oberflächenbereich des Schüttkegels Sedimentation auf. Mittels anschließender Verdichtungstechniken kann selbst bei visueller Kontrolle diese Sedimentation nicht effektiv beseitigt werden. Granulare Konvektionsströmungen können die Sedimentation sogar verstärken. Für Partikeldurchmesser-Verhältnisse größer als 7 können homogene Schüttdichten dadurch erreicht werden, dass die kleinen Partikel in die Zwischenräume der großen Partikel eingerieselt werden, die zuvor verdichtet und fixiert wurden. Schüttfaktoren von mehr als 84% wurden auf diese Weise erreicht. Diese spezielle Art binärer Schüttbetten wird jedoch derzeit für das EU Keramische Brutblanket nicht in Erwägung gezogen wegen eventueller Segregationseffekte bei zyklischem Blanketbetrieb. Weitere Untersuchungen sind notwendig um zu zeigen ob diese Effekte ein kritisches Problem darstellen.

Acknowledgements

Contents

1   Introduction

Granular materials enclosed in containers exist in numerous applications, such as silos in construction industry, grain elevators in food industry, blast furnaces for steel production, columns in chemical engineering processes, see e.g. [McG63], [Jes64], [Mar78]. Besides the necessity for knowing the amount of granular material in a given cavity, the distribution of the granular particles, especially those close to the container walls is of interest if granular materials are used for heat and mass processes.

In future nuclear fusion reactors with ceramic breeder blankets, granular materials, generally designated as pebble beds, play an essential role because both the ceramic breeder material and the beryllium, required as neutron multiplier, are used in form of pebbles. In these blankets, the pebbles are poured through small pipes in interconnected quasi-square cavities where one dimension, the pebble bed height H is much smaller than the other two dimensions, thus resulting in shallow pebble beds. Figure 1 shows the mock-up of the EU breeder unit with internal pebble bed volumes of Hx400x200mm, where H is 14,5 or 29mm. This mock-up was used for packing experiments [Abo08] simulating the beryllium bed with glass pebbles with d= 1mm. In other designs, H is in the range of 30 to 55mm [Her03]. For the Japanese blanket concept, special binary beryllium pebble beds are proposed [Eno98], consisting of mixtures of pebbles with large diameters $d_l \approx$ 2mm and small diameters $d_s \approx$ 0.2mm. The bed heights of the cavities for ceramic breeder materials in the EU breeder unit are in the range of 15-20mm; pebble diameters are between 0.25 and 0.65mm for orthosilicate (OSi) pebbles and between 0.8 and 1.2mm for lithium metatitanate pebbles.

Influence of the filling procedure: Large packing factors are desired in most technical applications and pebble beds need to be densified by technical means after filling the cavities. In most systematic investigations, cylindrical cavities were used (length L to diameter D ratio > 1) with a moveable lid (piston, weighted plunger) at the top. Different densification methods were applied: dropping the container for several cm [Wes30], using a vibrator [McG63], hammering the container walls [Dal00] or filling in the granular material with a small fall height to the bed surface [Jes64].

Multi-size pebble beds, consisting of pebble mixtures with several different pebble diameters, are of special importance because very high packing factors can be obtained. Most investigated were binary mixtures consisting of pebbles with two different nominal diameters (although in practice each group of pebbles has already a certain diameter variation). In this case, for diameter ratios of large to small pebbles of d_l/d_s > 7, the small particles can flow in the interstices of the large particles. Segregation effects are avoided by filling in first the large particles followed by densification. The large particles are then fixed, e.g. by a sieve (first proposed by [Aye65]) and the small pebbles fill the gaps between the large pebbles.
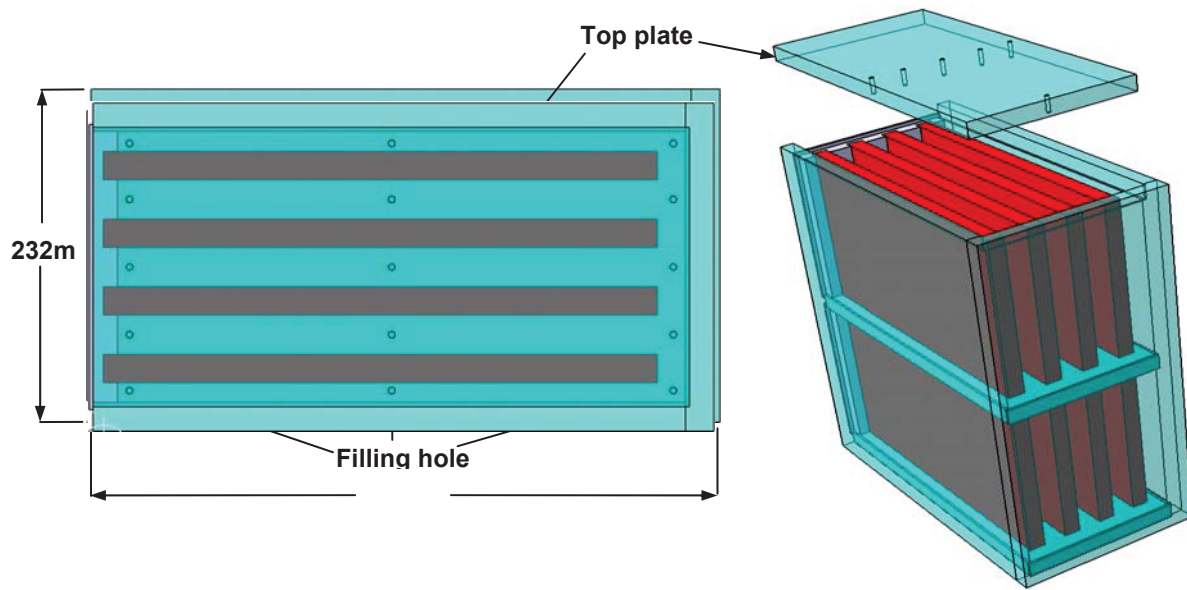
Fig. 1 EU breeder mock-up, from [Abo08].

With pebble ratios $d_l/d_s < 7$, segregation effects are difficult to avoid. One procedure [Wes30, Aye65] is to pour in again the large pebbles first, then, the small pebbles are layered on the top of the bed. The system is vibrated in such a way that the packing of the large particles is loosened in order that the small particles can enter the gaps in between. The other way is to use premixed (blended) material. The problem is to avoid segregation already within the filling reservoir. This effect plays a large role also in the pharmaceutical industry. Often, a third material is added in order to generate a paste and e.g. special screw mixers are used to homogenize the pebble diameter distribution [Pah85]. For the granular materials of interest in the present investigation, this method is not feasible.

If granular materials with a considerable particle size variation are poured in through openings at the top of the container, significant segregation effects occur because of sifting (Fig. 2a) or different repose angles (Fig. 2b), from [Sch09]. Subsequent vibration of pebble beds exhibiting free surfaces can easily cause granular convection flows which can either enforce or lessen segregation effects. However, this process is difficult to control.

In many technical applications, the pebbles must be often filled through small openings in an otherwise closed cavity. The achievement of a homogeneous and dense packing is not a trivial task even for single-size materials, as demonstrated by [Rei03] using a steel casing with dimensions of 100x100x15mm and a small filling pipe at the upper corner. One square plate served also as piston for subsequent uniaxial compression tests. By means of a pressure sensitive film at the inner side of this plate it was shown that a homogeneous pebble stress distribution was generally not reached (Fig. 3).
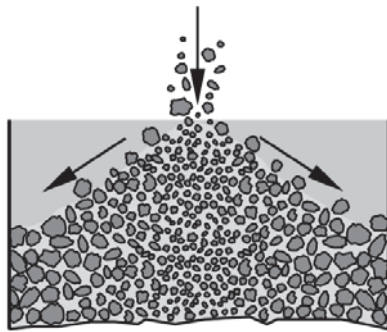
a) sifting: the fine particles concentrate under the point of impact while the larger particles roll off the pile.

kleiner
Böschungswinkel

großer
Böschungswinkel

a.

b.
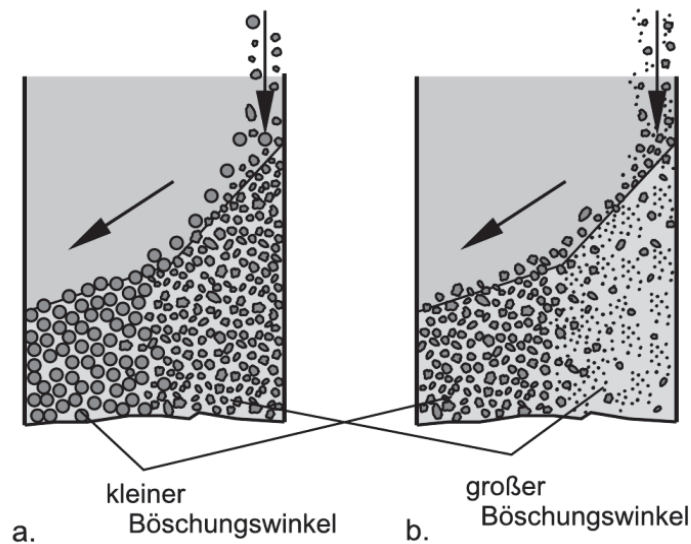
b) different repose angles: rough particles are characterized by larger repose angles compared to particles with a smooth surface (left hand side); very small particles have larger repose angles compared to large particles (right hand side)

Fig. 2. Segregation mechanisms [Schu09].

The EU breeder unit mock-up was also best filled through an opening at the highest location (Fig. 4). Stepwise filling and vibrating were applied. The use of Plexiglas walls was helpful for defining the optimum vibration parameters [Abo08].

Influence of particle shape and size distribution (large cavities): For a wide range of granular particles ranging from grain to coal, packing factors γ, defined as the ratio of volume occupied by the particles to the total volume, is between 60 to 64%, cf. e.g. [McG63].
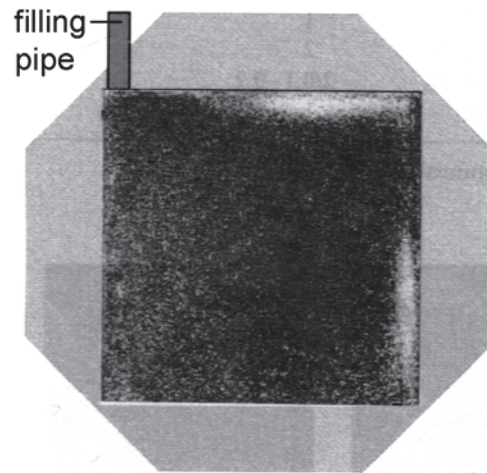
Fig. 3. Pebble bed stress distribution in square ducts [Rei03].
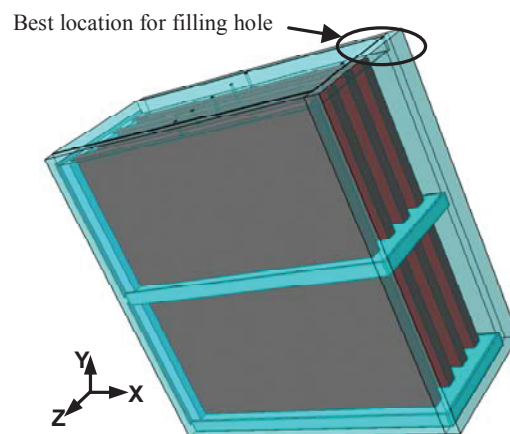
Fig. 4. Packing experiments with Breeder Unit Mock-up [Abo08].

Other detailed investigations with single-size spherical particles in large cylindrical cavities (diameter D/d » 10) by [Wes30], [McG63], [Jes64], [Aye65] resulted in packing factors between 62.5 and 63.5%. Although it was claimed by each author that the values are independent of sphere diameter and density, the differences indicate that a certain influence of the experimental parameters still exists. For the EU breeder mock-up a maximum value of γ =63.6% was obtained [Abo08] for 1mm glass spheres, which are also used in the present investigations.

Results for binary pebble beds from [McG63] are shown in Fig. 5. For the largest diameter ratios, values of $\gamma \approx 84\%$ were reached. The filling procedure of all experiments except that for a blended material

with the smallest diameter ratio of d_l/d_s = 3.44 consisted of pouring the small particles into the interstices of fixed large particles, as described above. Segregation effects could not be avoided.

Packing factors of $\gamma \approx$ 82% were reached for mixtures of 2 and 0.2mm diameter beryllium pebbles [Dal00], [Rei07b]. Owing to potential segregation effects during cyclic blanket operation, these binary beryllium pebble beds are presently not considered for the EU blankets.

Influence of container walls: Whilst in the pebble bed bulk no preferential orientation of pebble arrangements exist, a structured packing is observed in the vicinity of walls. The majority of the pebbles in the first layer adjacent to the wall are in contact with the wall and regions with regular pebble arrangements occur. With increasing number of layers, this regularity decreases and is no longer observed after about 5 layers. The structured packing in wall-neighbouring zones is characterized by fluctuations of the void distribution (void fraction = ratio of empty volume to total volume). Fig. 6 displays early results from [Ben62] with long cylindrical containers showing for the first time that with decreasing D/d the radial void fraction in the wall zone increases (and conversely the packing factor for the total volume decreases).
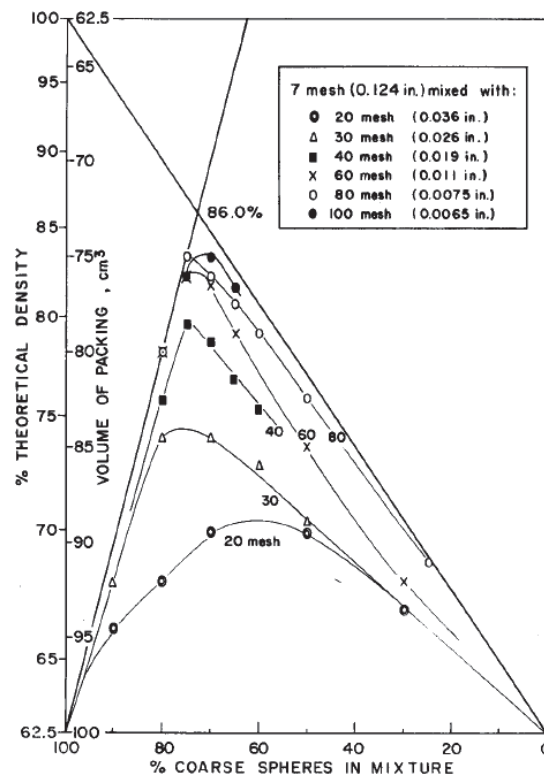
Fig. 5. Binary mechanical packing of a coarse steel shot with some other sizes [McG63].

Since then, many investigations have confirmed that the packing factors start to decrease with decreasing ratio D/d at values about 20. The void distributions shown in Fig. 6, measured in a quite complex way, were fitted by expressions containing cosines and exponential terms. However, already [Rid68] showed mathematically that more complex distributions should exist, see Section 2.
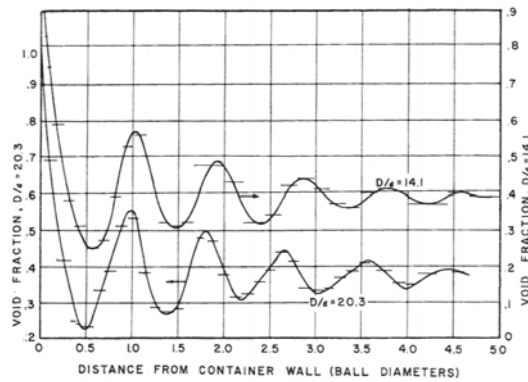
Fig. 6. Void fraction distributions in spherical pebble beds from [Ben62].

Many more details of both the arrangement of pebbles and the interaction of individual pebbles with neighbouring pebbles or walls were obtained in the last few years by three-dimensional (3D) computer aided microtomography (CMT) analyses of experiments performed at the European Synchrotron Radiation Facility (ESRF), Grenoble, France [Rei05,06b,07a, Pie11]. Besides evaluating void fraction distributions similar to those shown in Fig. 6, the position of each pebble in the container was determined as well as the number of contacts of the individual pebbles, the positions of these contacts on the pebble surface and even the sizes of the contacts, which are of special interest of interest for compressed pebble beds.

As an example, results of the experiment E0 with 2.3mm diameter aluminum spheres in a cylindrical cavity (D=49mm, H=46mm), compare Fig.10, are shown in Fig. 7 [Pie11]. The horizontal and vertical positions of the sphere centers are presented in graphs with the radial distance r and vertical distance as coordinates: the structured distributions with several layers at the cylindrical wall and at the bottom and
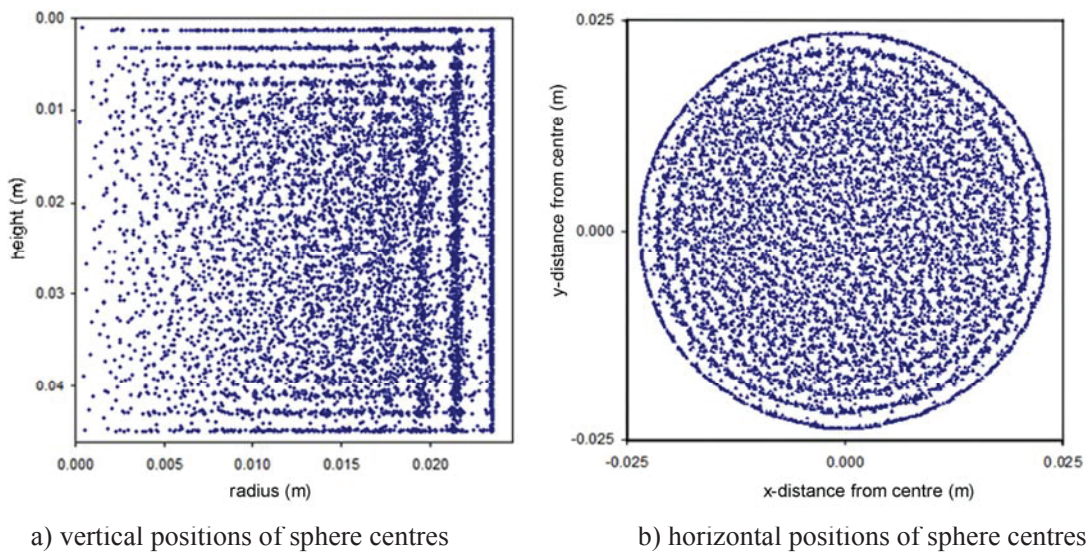
a) vertical positions of sphere centres   b) horizontal positions of sphere centres

Fig. 7. Vertical (a) and horizontal (b) positions of sphere centres (7768 elements) [Pie11].

top plates are clearly seen. A horizontal cut through the spheres in the first layer above the bottom plate is depicted in Fig. 8 (from [Pie11]): in the inner part, isles of hexagonal structure exist.
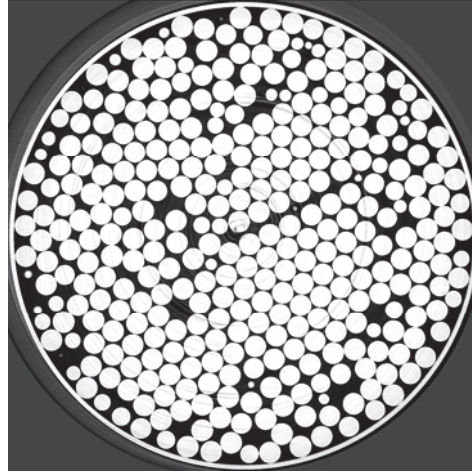
Fig. 8. Horizontal cut at z=1.5mm from the bottom of capsule E0 [Pie11].
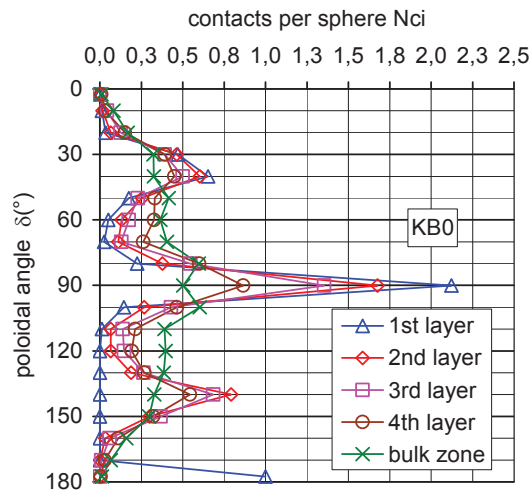
Fig. 9. Poloidal distribution of contact angles in the bottom plate zone [Rei07a].

Fig. 9, from [Rei07a] shows for a similar experiment the poloidal distribution of sphere contacts, N_{ci}, starting with $\delta=0°$ at the sphere north-pole. The 1st bottom layer exhibits peaks in the intervals $35° \leq \delta <45°$, $85° \leq \delta <95°$, and at $\delta \approx180°$. These peaks are characteristic for a hexagonal packing, where ideally three contacts exist at $\delta \approx 37°$ and six contacts at $\delta = 90°$. With increasing distance from the bottom, the hexagonal symmetry characteristics become less expressed but even in the 4th layer peaks are still present. For the bulk, the contact distribution approaches a cosine-type behaviour, which is the condition for homogeneously distributed contacts on the spheres.

2   New results of microtomographic investigations

Further analyses of the experiment E0 were performed, details of the experiments and the analytical methods are described elsewhere, see e.g. [Pie11]. Previous radial and axial void distributions were evaluated taking into account the total cavity volume. From Fig. 7 it is obvious that the characteristics of the axial void distribution should be evaluated more correctly using a cylinder that does not include the layers close to the cylindrical wall. Correspondingly, a cylinder without bottom and top layers should be better suited to evaluate the radial distribution.
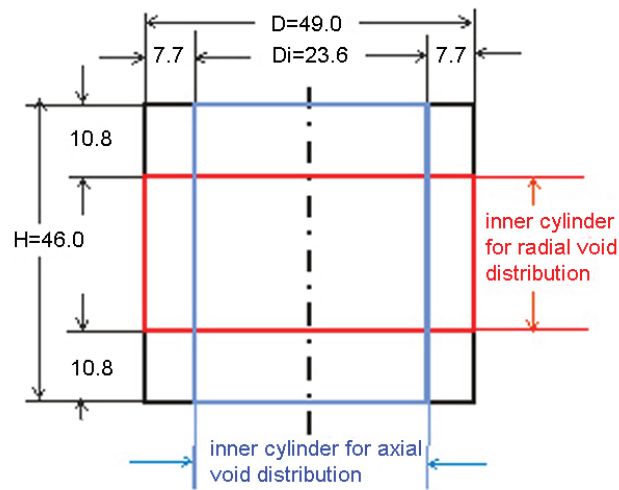
Fig. 10. Definition of inner cylinders.

Fig. 10 shows the resulting inner volumes. Different values were assumed for the thicknesses of the wall zones at the cylinder (4 layers with a total thickness of 7.2mm) and the bottom and top plates (6 layers with a thickness of 10.8mm). This fact takes into account that near flat walls the structured packing is more pronounced than near curved walls.

Figure 11a shows the axial distributions evaluated for the total ("..t") and inner ("..i") volumes: the values for the inner volume are distinctively smaller; the fluctuations close to the wall are more expressed. The differences in the radial distributions (Fig.11b) are negligible.

Fig. 12 shows void fraction distributions for the inner volumes as a function of the normalized wall distance z/d. The radial distribution is characteristic for the cavity diameter to sphere diameter ratio of D/d=21 whereas the axial distribution stands for the flat wall, D/d=∞. The void distribution for the flat wall is much more complex than that for D/d=21, caused by the fact that here structured packings are the most expressed. Applying the procedure of [Rid68] and using sphere wall coverage ratios ψ from the experiment, void distributions were calculated for the first wall layer both for D/d=21 and the flat wall, see

Fig. 13. For the flat wall, the calculated and measured distributions agree fairly well which again demonstrates that in this case predominantly a hexagonal packing exists.

The evaluation of axial and radial void fraction distributions for the different volumes allows also the determination of void fractions, respectively, packing factors, in characteristic zones, see Fig. 14. The packing factors of the bulk, bottom and top zones are very similar with values larger than 64%. The values in the cylindrical zone are about 60% in the corner regions and about 61 % in the middle zone.
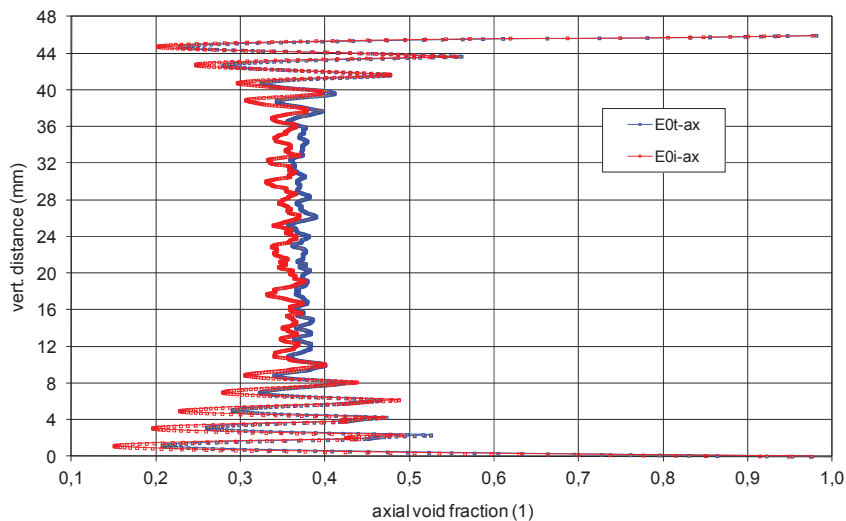
a. axial void fraction distributions
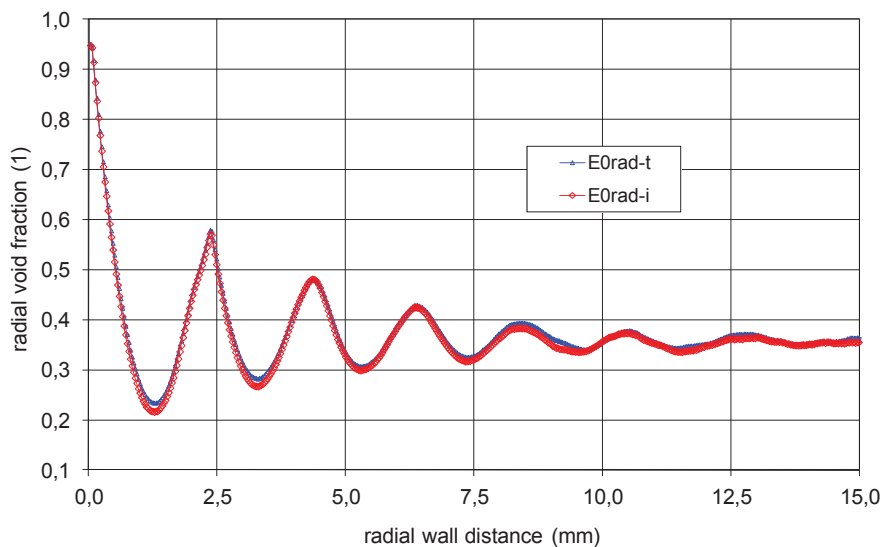
b. radial void fraction distributions

Fig. 11. Axial and radial void distributions in the total container volume and in its inner volumes.

The packing factor for the total volume is 62.3%. It should noted, that the value for the inner bottom zone is even slightly larger than that of the bulk, whereas at the top the value for the inner bottom zone is even slightly larger than that of the bulk, whereas at the top the value is smaller. The smaller value is caused by the fact that - during filling and subsequent densification - less pebbles can get in contact with the adjacent plate than in the bottom zone.
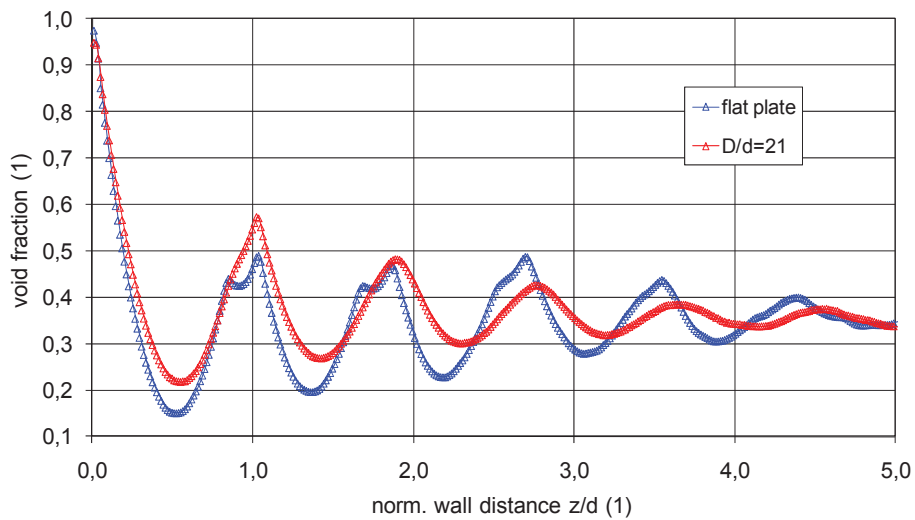
Fig.12. Void fraction distributions (inner volumes) for flat plate and cylindrical wall (D/d=21).
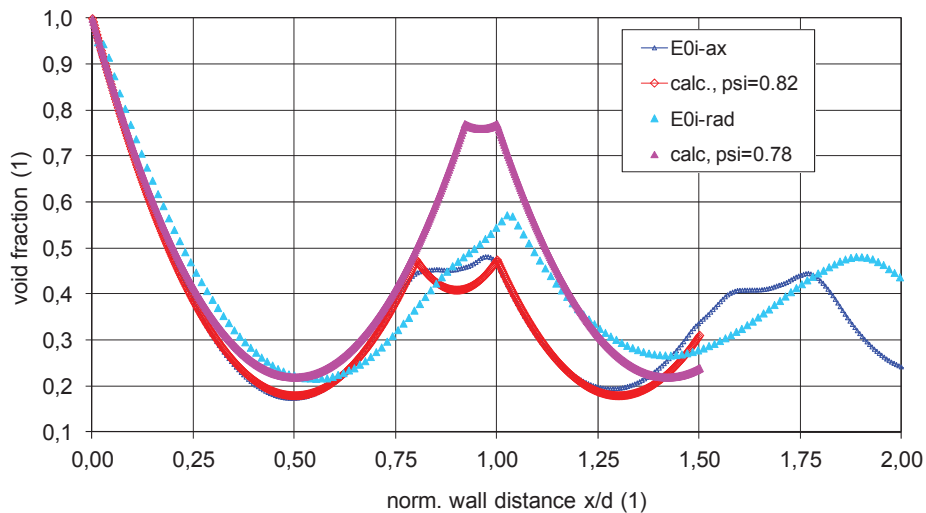
Fig.13. Measured and calculated void distributions for the first layer adjacent to a flat wall.
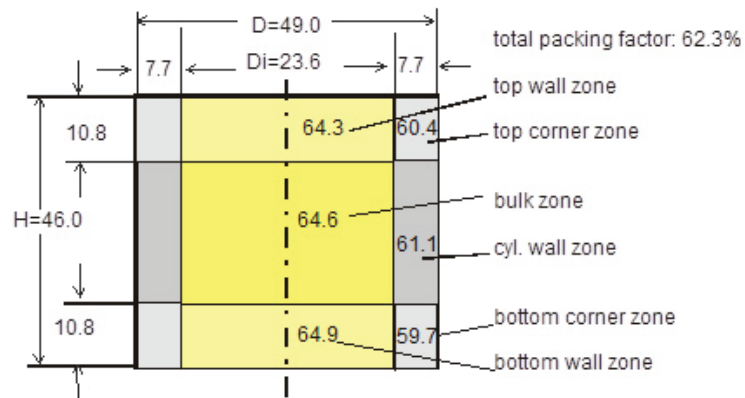
Fig. 14. Packing factors (%) in characteristic container zones.

The important conclusion from the present result is that the packing factor in wall zones decreases with decreasing D/d. For flat walls, the value can be about the same as for the bulk at least for mono-sized spherical particles. The reported results should not be extrapolated quantitatively to other experimental conditions e.g. to pebble beds consisting of particles with a distinct variation in size and shape. Further tomography investigations would improve considerable our understanding of these types of pebble beds.

3 Experimental work

3.1 Cavity geometries

The experiments were performed in the Karlsruhe Beryllium Handling Facility, KBHF, [Kur09]. The main goal was the measurement of packing factors with non-spherical beryllium grades. The limited amounts of these materials dictated the dimensions of the Plexiglas containers: the cylindrical container with $D = 50mm$, $H_{max} = 65mm$ and the square one with a volume of 100x100x10mm. In order to generate a broader data base, a square container with 100x100x20mm was also manufactured for the investigation of other granular materials, see Fig. 15. The cylindrical container was operated either by using a moveable piston at the top of the pebble bed (Type A cavity), or by fixing its dimensions (Type B cavity). With the arrangement of Type A, conventionally used in previous investigations, experiments with different bed heights H were performed. The Type B cavities are more representative for technical applications; both the cylindrical and square cavities were filled in tilted positions through a 4mm opening at the top corner.
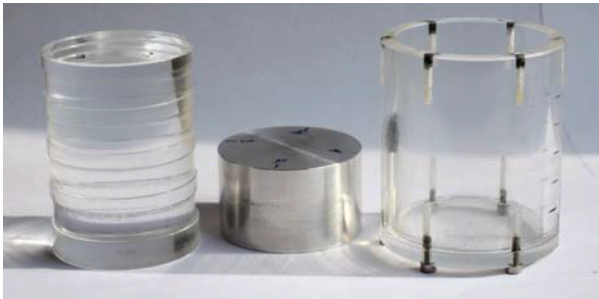
Type A container with different pistons   Type B containers

Fig.15. Container geometries.

3.2 Granular materials

Table 1 lists characteristics of the investigated granular materials; photographs of pebbles are shown in Fig. 16. Before channelling the experimental set-up into the glove-box required for the beryllium experiments, investigations were performed with glass, steel and lithium orthosilicate (OSi) spherical particles. The OSi experiments were carried out using an argon purged plastic glove-box in order to avoid the uptake of humidity.

Material	nominal diameter d(mm)	diameter distribution (mm)	material density (g/cm3)	pebble/ Material density (%)	morphology
glass 0.4	0.4	0.25 - 0.65		100	spherical, smooth
glass 0.65	0.65	0.55 - 0.75		100	
glass 1.0	1.0	0.85 - 1.25		100	
OSi 0.3	0.3	0.25-0.65		95	spherical with indentations
steel 2.0	2.0	2+-0.05		100	spherical, smooth
steel 4.0	4.0	4+-0.05		100	
beryllium 1	1.0	0.8 -1.2		98	spherical with indentations
beryllium A	1			98	nonspherical; crushed material with rounded edges
beryllium B	1.5			98	
beryllium C	1.5			98	
beryllium D	1.5			98	

Tab. 1.: Single-size granular materials.

Five different beryllium batches were investigated: nearly spherical pebbles with a mean diameter of 1mm used also in previous investigations, see e.g. [Rei06a], produced by NGK, Japan, via the rotating electrode process (Be-1), and four materials manufactured by crushing sintered beryllium blocks and subsequent grinding. As a result, non-spherical pebbles are fabricated and the values of the largest pebble dimension reach up to 2.5mm. As a characteristic diameter, a value of 1.2mm is assumed. The batches Be-A, B, and C were produced by Bochvar Institute, Russia, and differed in grain size. The batch Be-D originated from Materion, USA, formerly Brush Wellman. The very small available amount of this material restricted however the range of experiments.
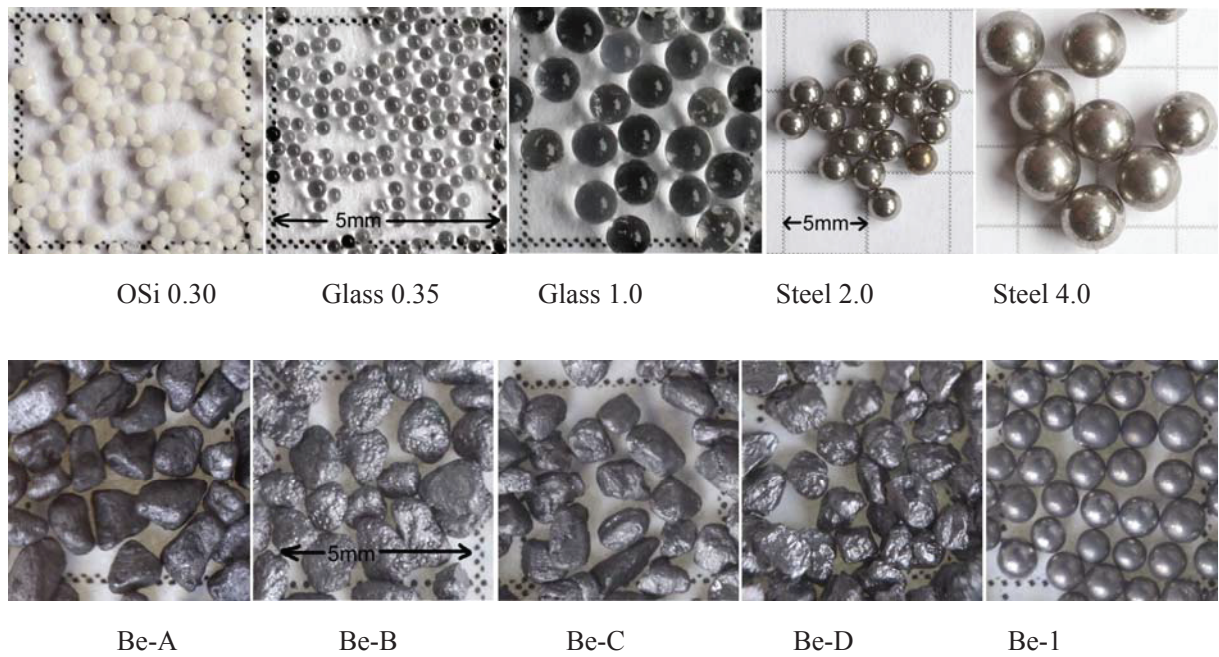
Fig.16. Pebble images.
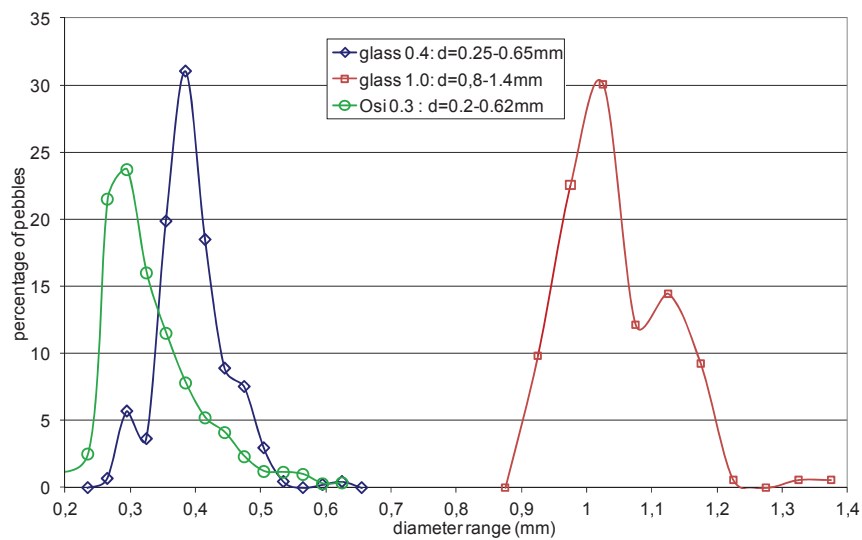
Fig.17. Size distribution of some granular materials.

The size distribution of some of the used materials is shown in Fig. 17. The batches are denominated according to their mean diameters, and are considered as single-size batches in order to differentiate them from mixtures of these which are named as multi-size materials. The diameters of the steel spheres deviate only marginally from the nominal diameter. The 2mm steel spheres were selected because the experimental parameters are close to those of the previously discussed experiment E0. The 4mm steel pebbles

resemble those used in former tomography experiments (not mentioned in this report). In this case, the D/d value is so small, that a bulk zone no longer exists.

It should be reminded here that the packing factor γ, defined as the ratio of volume occupied by the pebbles, $V_{pebbles}$, to volume of the cavity, V_{cavity}, and is given by

$$\gamma(1) = V_{pebbles}/V_{cavity} = m_{pebble\ bed}/((1-P)\rho V_{cavity}),$$

where $m_{pebble\ bed}$ is the total mass of pebbles, ρ is the density of the pebble material, and P is the

a: Definition of repose angle
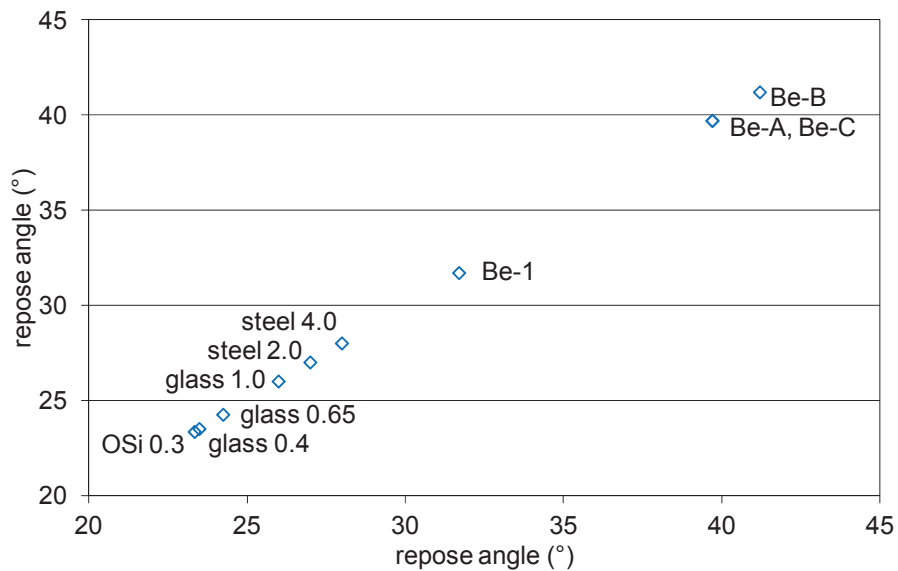
b: Results

Fig.18. Repose angles of the investigated materials.

porosity of the pebbles. Whilst for the glass and steel spheres a porosity P = 0 was assumed, P = 0.05 was used for the OSi pebbles as found by Hg porosity measurements [Kni07] and, for Be-1, P = 0.02, as used previously. For the other Be batches, P = 0.02 was also assumed.

Fig. 18b displays results of the repose angle of some batches, measured after pouring the granular materials in a square cavity, see Fig. 18a. The repose angle is a measure of the pebble friction and is expected to influence the pebble bed packing. The repose angle β generally increases with increasing surface roughness, irregular shape, and particle size. The smooth spherical glass spheres show values between 23.5-26°, a value of β ≈ 28° for the rather spherical 1mm Be pebbles was found and the strongly irregular pebble shapes of Be-A, B, and C resulted in values of about 40°.

Table 2 shows that also mixtures of the materials listed in Table 1 were investigated. These materials were either blended before filling or the large spheres were first poured in and then the small ones.

Granular material	Filling
glass 0.35 + 0.65	blended
glass 0.35 + 1.0	
glass 0.35 + 0.65 +1.0	
steel 2.0 + 4.0	
steel 2.0 + glass 0.35	separate
steel 4.0 + glass 0.35	

Table 2. Multi-size granular materials (equal volume fractions).

In order to obtain dense packs, energy must be introduced into the system by knocking the container walls or vibrating the containers to such an extent that pebbles can overcome frictional forces with neighbouring pebbles in order to find positions with the smallest potential energy. For vibration, a vibration table (Renfert Vibrax Vibrator M-13295) was used which operated at (230 V / 50 Hz) with different amplitudes.

4　Results

4.1　Densification techniques

Filling the containers by a funnel resulted in non-densified pebble beds with packing factors of about 59%. Densification of the bed can be achieved either with i) a free pebble bed surface (Type A cavity without piston or stepwise filling of a Type B cavity) or ii) without a free surface (Type A cavity with piston or initial complete filling of a Type B cavity).

The segregation issue of densification by vibration of multi-size pebble beds was already mentioned before. However, densification via vibration poses also problems for single-size granular materials if the vibration energy is large enough to cause granular convection. Convection flows can happen only in loosened pebble beds, hence, a priori, a dense packing does not exist in these zones.

In pebble beds with a free surface, the vibration energy required for convection flow generation increases with decreasing fraction of the free surface to the surrounding wall surface. If, for instance Type B cavity is filled in the tilted position to about 50%, a small vibration energy is sufficient to generate a convection flow in almost the complete pebble bed, see Fig.19. For the same vibration parameters and a filling of 90%, the convection flow restricted to a very small zone at the top.

Fig.19. Granular convection flow.

Despite of the detrimental effect of convection flows described above, these flows can be helpful under controlled conditions to generate dense packs, especially in large cavities of Type B. Stepwise filling is

recommended; for each filling level, the convection flow should be adjusted stepwise in such a way that the flow region becomes smaller and shifts upwards. The idea is that at the lower border of the convection region the pebbles can achieve dense arrangements of positions.

The alternative to densification by vibration is hammering/knocking against container walls. Again, similar problems occur: in order to affect the lower part of the pebble bed, energies are required which, on the other hand, cause a pebble bed loosening in the upper part.

In the present experiments, a combination of vibration and knocking was generally applied. The parameters could be visually controlled, and the obtained packing factors are generally larger than in previous investigations where often steel containers were used, see e.g. [McG63]. The values obtained are probably at the upper limit of the range of values achievable in large blanket components

The above statements emphasize that it is not possible to recommend unique densification parameters for large pebble bed containers. Even for a given container, the parameters depend on the filling level, and relevant pre-tests are highly recommended.

4.2 Pebble bed packing characteristics

For visualization of pebble structures, the steel spheres were best suited. Fig. 20 shows 2mm spheres in the Type A cavity after densification: hexagonal structures of the layers at the cylindrical wall and bottom plate are well developed; ordered structures at the top plate (piston) exist to a much lesser extent. During filling, the spheres at the bottom plate arrange already in a quite close-packed array; densification enforces then this tendency. At the pebble bed top, the pebbles, except those in the cylindrical wall layer, arrange irregularly after filling, like those in the bulk zone. With the movable piston on top of the bed and subsequent densification, the generation of contacts with the upper wall is favoured and, to a smaller degree, also the development of regular structures. In Fig. 20, the differences in the wall layers can be seen.

a) cyl. wall layer   b) bottom plate layer   c) top plate layer
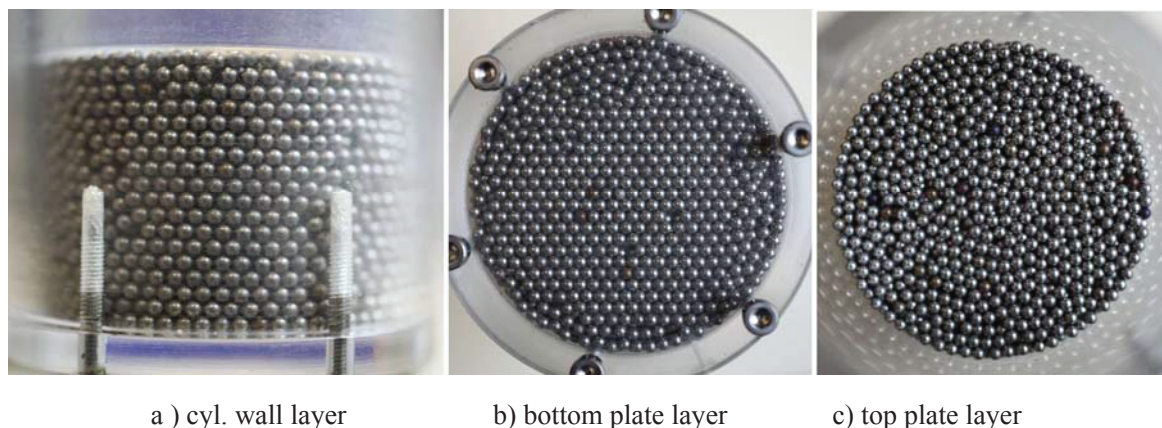
Fig. 20. Cylindrical cavity, H = 32.5mm, 2mm steel spheres, γ = 63.85%.

Results for the square cavity are presented in Fig. 21: the denser packing is visible at the bottom sides 2 and 3, as compared to the top sides 1 and 4. For a blanket breeder unit, side 2 would correspond to the First Wall; a dense packing would promote heat transfer.
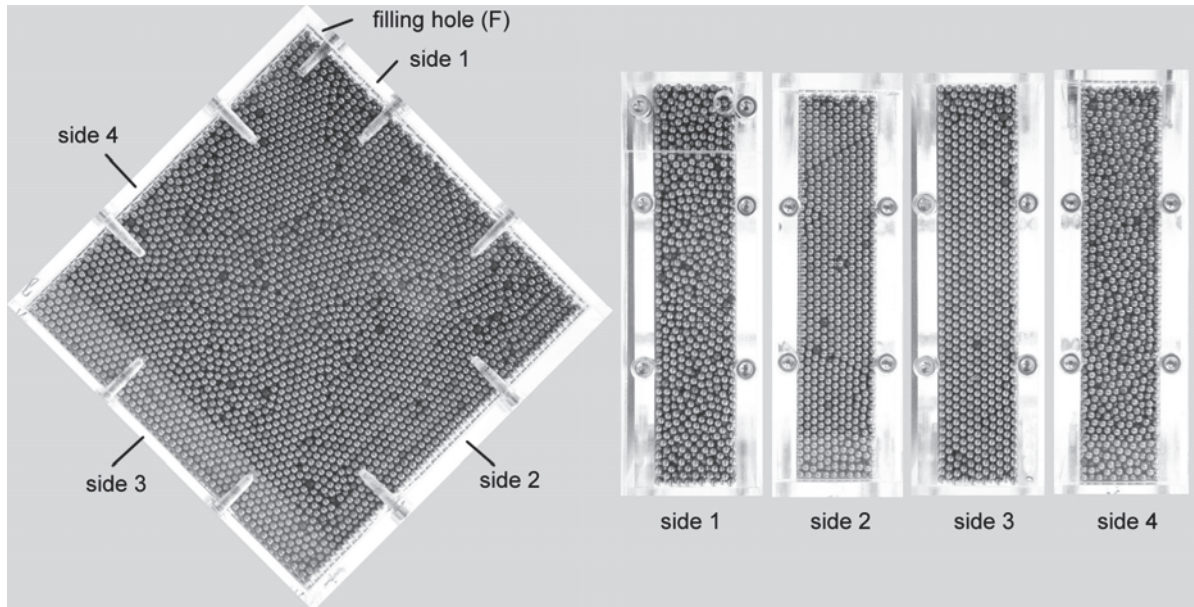
Fig. 21. Square cavity, H = 20mm, 2mm steel spheres, $\gamma = 64.19\%$.
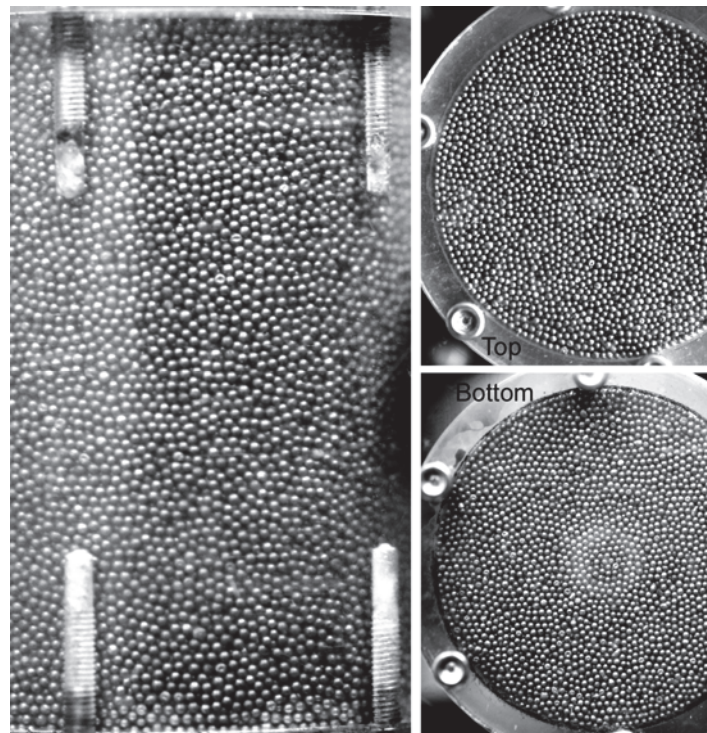
Fig. 22. Cylindrical cavity, H = 65mm, Be-1, $\gamma = 61.85\%$.

The next figures contain photographs of beryllium batches. The pictures were taken through the Plexi-glas glove-box pane, therefore, the quality is worse compared to the previous figures. Figures 22 and 23 show cavities filled with Be-1. Although these pebbles are quite spherical, regular patterns are much less
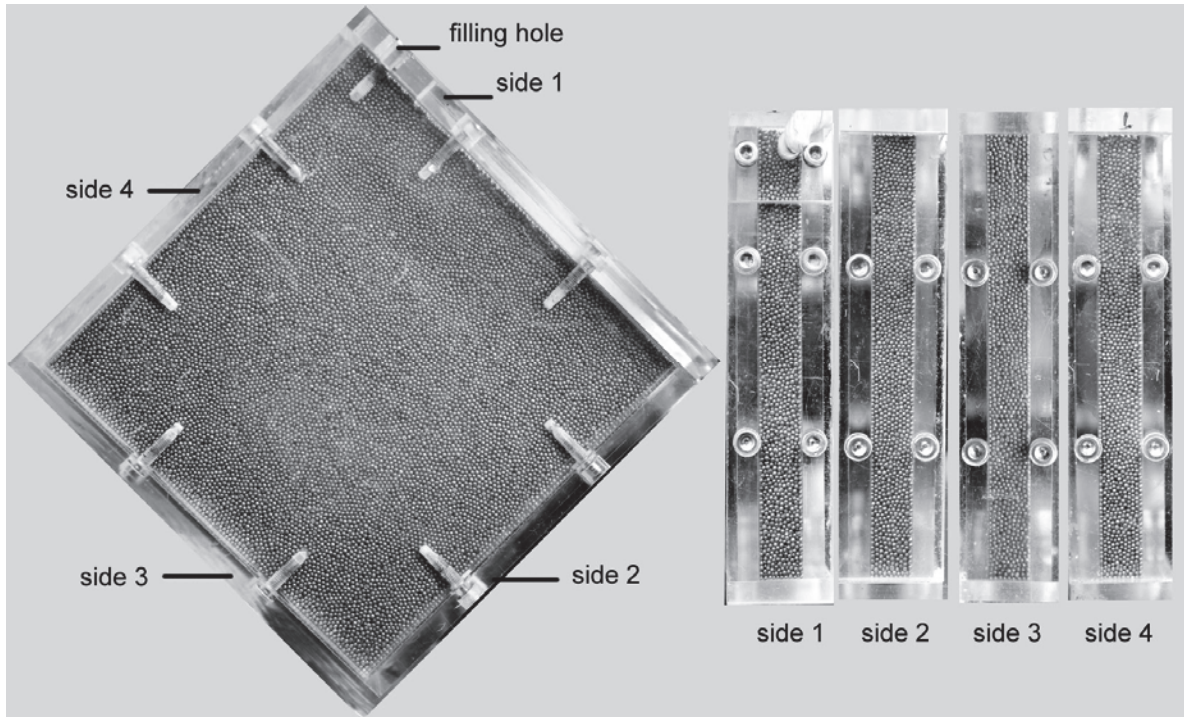
Fig. 23. Square cavity, H = 10mm, Be-1, γ = 62.19%.
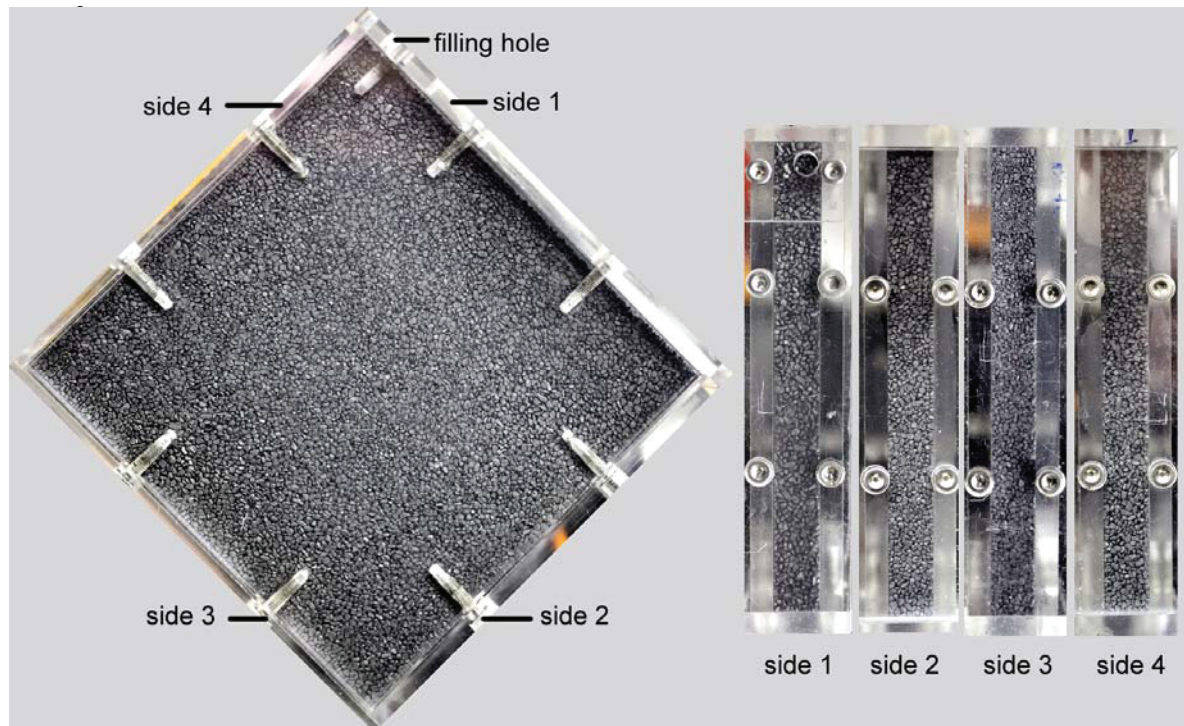
Fig. 24. Square cavity, H = 10mm, Be-A, γ = 62.0%.

pronounced than for the steel spheres. The visual differences between the different cavity sides are much smaller, see Fig. 23. One reason for the smaller regularity of the Be-1 pebbles might be the significantly larger diameter variation with respect to the steel spheres.

Fig. 24 shows the non-spherical particles Be-A in the square cavity. Regular pebble arrangements are not detected, however, the particles tend to align their largest side along the wall. This fact is also considered as structured packing; the question is to which extent this tendency also exists in the next inward wall layers. Tomography experiments with this type of pebbles would allow measuring void fraction distributions and determining local packing factors for the wall and bulk zones. It should be noted that the largest particle size preferentially being in contact with the wall is expected to be beneficial for heat transfer.

Fig. 25 a) and b) show examples for blended multi-size glass sphere beds. Segregation occurred because i) segregation existed already in the filling bottle, and ii) according to the sifting effect, see Fig. 2. Although the effectiveness of vibration parameters was controlled visually, segregation could not be avoided completely.

Fig. 26a) shows a binary bed consisting of 4mm steel and 0.35mm glass spheres, $d_l/d_s = 11.4$, where, first, the large steel spheres were poured into the cavity and densified until particle movement no longer occurred. Then, the glass spheres were poured in through the small opening and vibrated. At one container corner, a gap was formed during this vibration period, therefore, the filling is not complete. The container failure is an indication for the occurrence of large forces during vibration of binary beds with large d_l/d_s ratios. In experiments with similar binary beryllium experiments, pressures of 6MPa were measured at the container walls [Gor12].

a)   b)
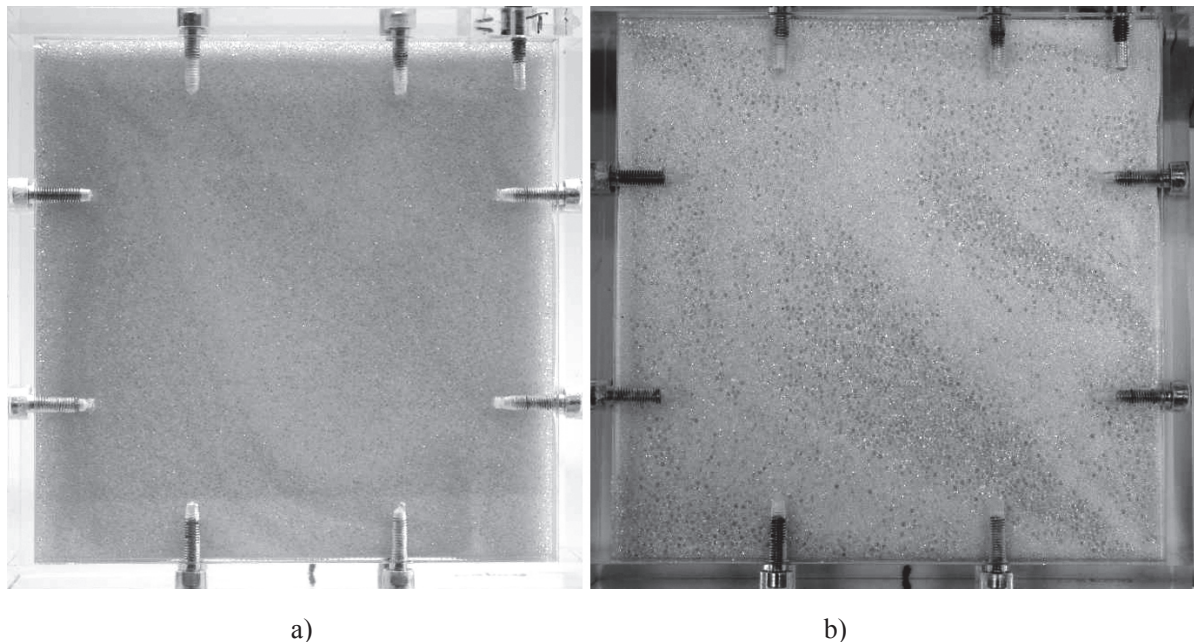
Fig. 25. Binary pebble beds; a) glass spheres, $d_l = 0.65$mm, $d_s = 0.35$mm, $\gamma = 65.0\%$; b) glass spheres, $d_l = 1.0$mm, $d_s = 0.35$mm, $\gamma = 67.7\%$.

<center>a)   b)</center>
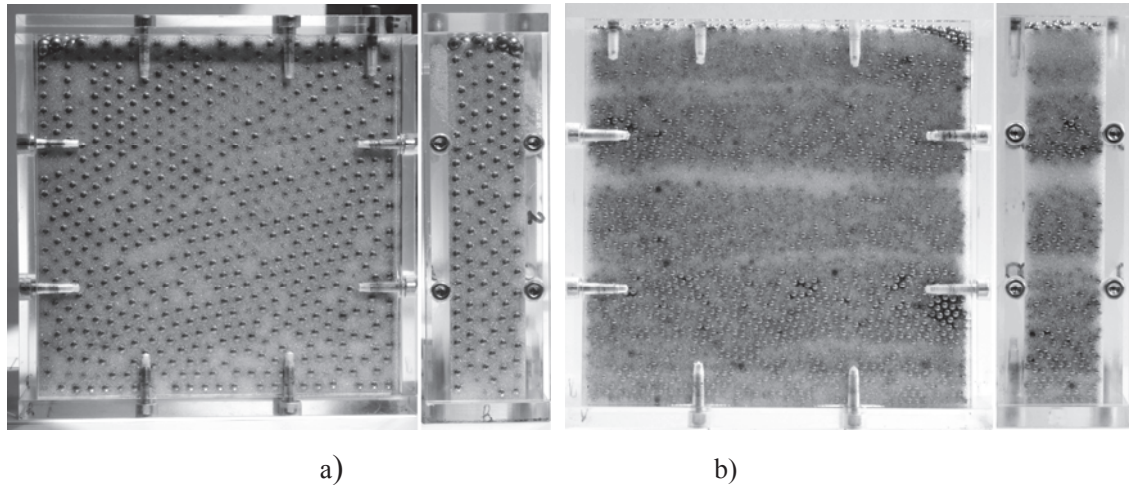
Fig. 26. Binary bed with a) 4.0mm steel spheres and 0.35mm glass spheres, b) 2.0mm steel spheres and 0.35mm glass spheres.

The binary bed consisting of 2mm steel and 0.35mm glass spheres was generated in a different way: First, the container was filled to about 30% with the steel spheres, then, covered with a layer of glass spheres. A modest vibration caused the movement of the small spheres in the gaps between the large spheres. This procedure was repeated several times until the container was completely filled. No homogenous filling was obtained as can be seen in Fig. 26b.

4.3 Packing Factors

4.3.1 Packing factors of single-size granular materials

Fig. 27 shows packing factor versus pebble bed height results for spherical pebbles in a cylindrical cavity. As mentioned before, all experiments were performed with a piston on top of the pebble bed (Type A cavity) except for H=65mm, where the top plate was fixed (Type B cavity). For pebble diameters d ≤ 1mm, the ratio D/d is ≥ 50. With this, the cylinder wall should hence play a negligible role, except for the 4mm steel spheres. The data should thus be representative for shallow pebble beds and the relevant parameter is the H/d ratio. However, the previous statement, that below D/d ≈ 20 a wall effect occurs, resulted from experiments with long cylinders. For decreasing H, the corner zones have an increasing influence, cf. Fig.14. Therefore, the result for the 2mm steel spheres at H=10mm might be influenced by this effect. The same holds even more for the 4mm steel spheres, where an expressed bulk zone does not exist at all H.

For pebble diameters d ≤ 1mm, there is a weak tendency for γ to increase with decreasing H. This tendency differs characteristically from that found in long cylinders where D/d is the characteristic parameter. With decreasing H, the bulk zone becomes smaller and the influence of the flat wall zones increases.

The moveable top plate favours also the development of structured packs at the top wall, which is associated with a large local packing factor, cf. Fig.14.

Fig. 27 Single-component packing factors for cylindrical cavities with different heights.

At large H, the obtained packing factors are generally larger (exception: 4mm steel sphere beds) than those reported by [McG63]. The reasons for this can be i) more efficient densification procedures, and/or ii) the fact that most "single-size" materials consist of pebbles with a larger size spread than those used by [McG63].

Fig. 28. Single-size packing factors for H = 10 and 20mm for cylindrical (left) and square (right) cavities.

Packing factors of the OSi pebble and the 0.35mm glass sphere beds are about the same. Both pebble batches have a similar diameter spread and repose angle, see Figs. 17 and 18. The present OSi values agree very well with those defined previously as reference values [Rei04]. For Be-1, γ is about 62.5% [Rei06a]. This value is about 1% smaller than the comparable 1mm glass pebble bed. The difference is attributed to the rougher surface of the Be pebbles and the smaller sphericity.

The maximum height H = 65mm belongs to the Type B cavity. The packing factors are similar to those for large bed heights with the piston on the top.

Fig. 28 shows results for H=10 and 20mm both for the cylindrical Type A cavity and the square Type B cavity. Fixed cavity walls partly result in less dense packs, as shown in Section 4.2, thereby lower packing factors are expected in square Type B cavities. This is generally found for the H=10mm cavity but to a much smaller extent for the 20mm cavity; see e.g. the results for Be-1. However, for square cavities with H in the range of 30mm or more, used in present HCPB blanket designs, the packing factor for Be-1 is expected to reach the reference value of 62.5%.

For OSi, packing factors of about 64.5% were obtained in both square cavities. The H/d ratio is considerably larger than 10 for the 10mm cavity, furthermore, the small repose angle might promote the formation of dense packs in small closed cavities. This is an important result because in several blanket designs bed heights between 10 and 20mm are considered.

The packing factors for the 2mm steel spheres are also surprisingly high in the 20mm cavity, although H/d is only 5, probably caused by the very regular packing in the wall zone, cf. Fig. 21.
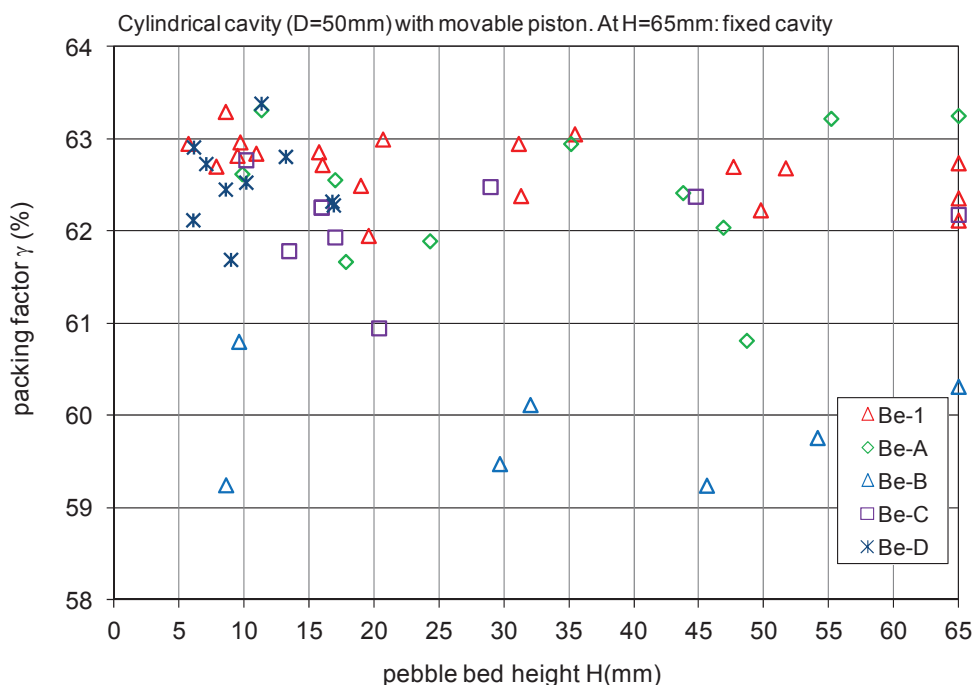
Fig. 29. Packing factors for different granular beryllium materials in cylindrical cavities.

Fig. 29 shows results for the different beryllium grades in the cylindrical cavity. The mean packing factors for all materials, except Be-B, are very similar although repose angles differ considerably between Be-1 and the other grades. One reason might be the formation of dense wall layers by the irregularly shaped pebbles owing to the fact that these particles tend to align their largest side along the wall, see Fig. 24. As mentioned before, densification with the movable piston might favour this formation. The low values for Be-B can be explained in different ways: i) this grade has a much rougher appearance than the other grades, confirmed by the largest repose angle, see Figs. 16, 18b. This large roughness was probably caused by a non-perfect sintering process [Kur12] which also could result ii) in a larger value of the pebble porosity than that assumed for all beryllium grades.
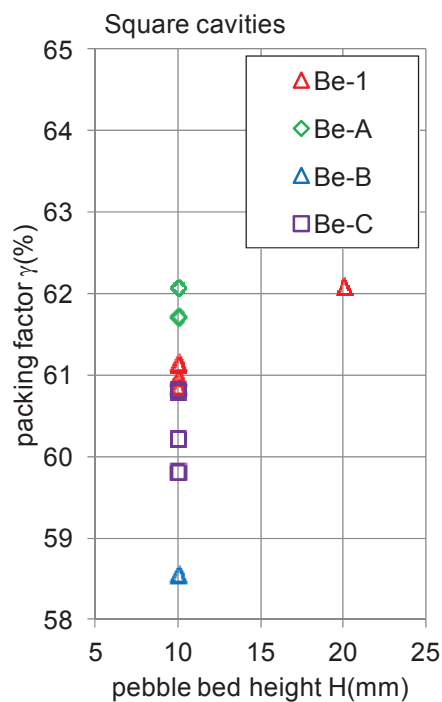
Fig. 30. Packing factors for different granular beryllium materials in square cavities.

Figure 30 shows results for the square cavity. The available amounts of Be-A, B, and C sufficed just to fill the 10mm cavity. As observed for the spherical pebbles, the packing factor in the cavity with fixed walls is smaller than that with the movable wall. Again, it is expected that with increasing bed heights the packing factor increases, as for Be-1.

4.3.2 **Packing factors of multi-size granular materials**

Results for multi-size particle mixtures in the cylindrical Type A cavity are shown in Fig. 31. As mentioned before, packing factors should increase with increasing ratio of d_l/d_s. All experiments were performed with blended materials, therefore, segregation effects could not be avoided. For the mixtures of 0.35 + 0.65mm, and 0.35 + 1mm glass spheres, packing factors of 66 and 69%, respectively, were obtained. These values are below those calculated by the correlations proposed by [Jes64], i.e. 67.3 and 69.4%, respectively. For a ternary mixture of glass spheres, also a packing factor larger than that of a single component pebble bed was found; again, significant segregation effects were visible.
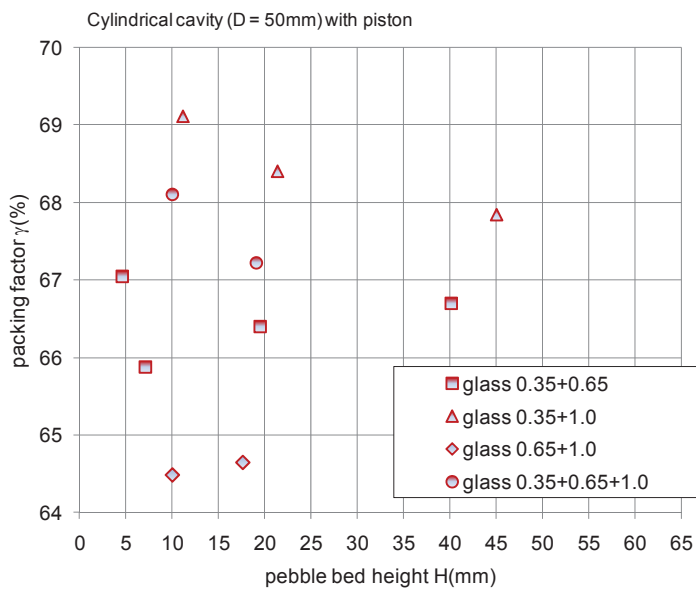
Fig. 31. Multi-size packing factors for cylindrical cavities.
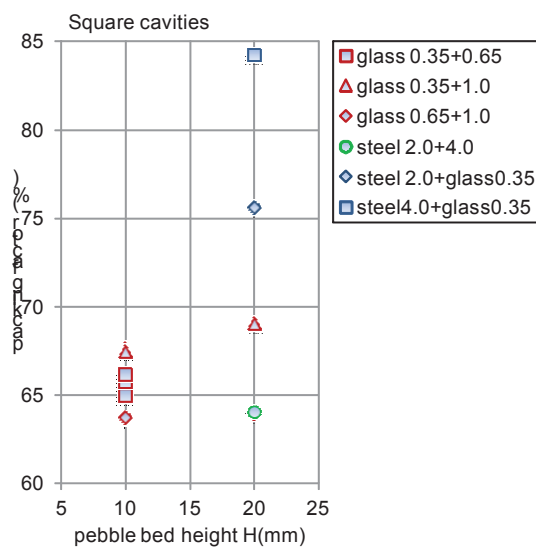
Fig. 32. Multi-size packing factors for square cavities.

Results for the square cavities are presented in Fig. 32. Filling up the containers with blended material through the small opening causes even stronger segregation because of the sifting effect. As a consequence, the packing factors are smaller compared to the cylindrical cavity. For the binary beds with steel and glass pebbles, produced as described in Section 4.2, $\gamma = 84.2\%$ was obtained for the 4mm steel and 0.35mm glass sphere bed which agrees well with the results shown in Fig. 5. The value of $\gamma = 75.6\%$ for 2mm steel and 0.35mm glass sphere bed is lower due to significant segregation effects.

5   Conclusions

The objective of the present investigations is to determine packing factors in cavities with flat walls and bed heights relevant for both ceramic and beryllium pebble beds in combination with blanket-relevant filling conditions.

In the past, packing factor experiments focused mainly on cylindrical cavities and a decrease of the packing factor with decreasing ratio of cylinder diameter to pebble diameter was observed. In cavities with flat walls and small widths (bed heights H), the ratio H/d is the relevant parameter.

New analyses of recently performed tomography investigations at the European Synchrotron Radiation Facility (ESRF) showed quantitatively that for flat walls packing factors in the wall zone are as high as in the bulk zone, in contrast to the values obtained near cylindrical walls and corner zones.

Experiments with a cylindrical cavity and a movable piston on the top showed the tendency of the packing factor to even increase slightly with decreasing bed height. This was attributed to the fact that for this experimental condition, the development of structured packs close to the flat walls is favoured.

The experiments with closed square cavities indicated that for both beryllium and OSi pebble beds the reference values of the packing factors obtained in large cavities are reached for blanket-relevant bed heights (10-20mm for OSi and 30mm or more for beryllium).

Whereas most pebble grades had rather spherical shapes, the experiments with granular beryllium were performed with five different batches: the reference material with almost spherical 1mm diameter pebbles and four other grades with quite irregular shapes and a characteristic diameter of about 1.2mm, originating from crushed beryllium blocks. The results for the reference materials and three other grades behaved very similarly for all experimental parameters, although, visually the wall layers looked quite different.

Further experiments with the non-spherical materials are required in order to judge if these materials could be candidates for blankets; the next steps should be uniaxial compression tests and thermal conductivity measurements.

Additional tomography experiments would increase considerably the understanding of the morphology and topology of these pebble beds.

6   References

[Abo08] A. Abou-Sena, H. Neuberger, T. Ihli, Experimental investigation on the possible techniques of pebbles packing for the HCPB Test Blanket Module, Fusion Engineering and Design 84 (2009) 355-358.

[Aye65] J.E. Ayer, F.E. Soppet, Vibratory compaction: I, Compaction of spherical shapes, J American Ceramic Society, Vol. 48, No. 4, (1965) 180-183.

[Ben62] R. F. Benenati, C. B. Brosilow, Void fraction distributions in beds of spheres, A.I. Ch. E. Journal, Vol. 8, No. 3, (1962) 359-361.

[Dal00] M. Dalle Donne, A. Goraieb, G. Piazza, F. Scaffidi-Argentina, Measurements of the heat transfer parameters in infiltrated binary beryllium pebble beds. Comparison between results with PEHTRA and SUPER-PETRA, Fusion Technology, Vol. 38, No. 3, (2000) 310-319.

[Eno98] M. Enoeda, K. Furuya, H. Takatsu, S. Kikuchi, T. Hatano, Effective thermal conductivity measurements of the binary pebble beds by hot wire method for the breeding blanket, Fusion Technology, Vol. 34, No. 3, Pt. 2, (1998) 877-881.

[Gor12] A. Goraieb, personal communication, 2012.

[Her03] S. Hermsmeyer, B. Dolensky, J. Fiek, U. Fischer, C. Köhly, S. Malang, P. Pereslavtsev, J. Rey, Z. Xu, Revision of the EU Helium cooled pebble bed blanket for DEMO, 20th SOFE, San Diego, USA, Oct. 14-17, 2003, Piscataway, N.J. : IEEE, (2003) 440-445.

[Jes64] R. Jeschar, Druckverlust in Mehrkornschüttungen aus Kugeln, Archiv für das Eisenhüttenwesen, 35. Jg., Heft 2, Feb. (1964).

[Kni07] R. Knitter, B. Löbbecke, J. Nucl. Mater. 361 (2007) 104–111.

[Kos99] V. Y. Koshelev, Spherical superalloy powder segregation using large-sized can filling for subsequent HIPping, Proc. Int. Conf. Hot Isostatic Pressing, 9-11 June, 1999, Bejing, China, 87-97.

[Kur09] P. Kurinskiy, V. Chakin, A. Moeslang, R. Rolli, A.A. Goraieb, H. Harsch, E. Alves, N. Franco, Characterisation of titanium beryllides with different microstructure, Fusion Engineering and Design 84 (2009) 1136-1139.

[Kur12] P. Kurinskiy, personal communication, 2012.

[Mar78] H. Martin, Low Peclet Number particle-to-fluid heat and mass transfer in packed beds, Chem. Eng. Science Vol.33, (1978) 913-919.

[McG63] R. K. Mc Geary, Mechanical packing of spherical particles, J. Am. Ceram. Soc.,Vol. (1963) 514-522.

[Pah85] M. Pahl, Mischen in Schneckenmaschinen, Teil 1: Homogenisieren, Chemie Ingenieurtechnik 57(5) (1985), 421-430.

[Pie11] R. A Pieritz, J. Reimann, C. Ferrero, 3d Tomography Analysis of the Inner Structure of Pebbles and Pebble Beds, Advanced Engineering Materials, 13, No.3, (2011), 145-155.

[Rei03] J. Reimann, D. Ericher, G. Wörner, Influence of pebble bed dimensions and filling factor on mechanical pebble bed properties, Fus. Eng. Design 69 (2003), 241-244.

[Rei04] J. Reimann, G. Harsch, Characterization of orthosilicate ex hydroxide pebble beds and mechanical cycling of different types of ceramic breeder materials, 12th Intern. Workshop on Ceramic Breeder Materials, Karlsruhe, Germany, Sept. 16-19, 2004, FZKA 7078.

[Rei05] J. Reimann, R. A. Pieritz, M. di Michiel, C. Ferrero, Inner structures of compressed pebble beds determined by X-ray tomography, Fusion Engineering and Design 75 – 79 (2005) 1049 - 1053.

[Rei06a] J.Reimann, G. Piazza, H. Harsch, Thermal conductivity of compressed beryllium pebble beds, Fusion Engineering and Design, 81 (2006), 449-54.

[Rei06b] J. Reimann, R.A. Pieritz, R. Rolli, Topology of compressed pebble beds, Fusion Engineering and Design, 81(2006), 653-58.

[Rei07a] J. Reimann, R.A. Pieritz, C. Ferrero, M. di Michiel, R. Rolli, X-ray tomography investigations on pebble bed structures, Fusion Engineering and Design 83 (2008) 1326 – 1330.

[Rei07b] J. Reimann, A. Goraieb, H. Harsch, Thermal Conductivity of Compressed Binary Beryllium Pebble Beds, Proc. 8th Int. Workshop on beryllium Technology, Lisbon, Portugal, Dec. 5-7, 2007.

[Rid68] K. Ridgway, K. J. Tarbuck, Voidage fluctuations in randomly-packed beds of spheres adjacent to a containing wall, Chem. Eng. Science, Vol. 23, (1968) 1147-1155.

[Sch09] D. Schulze, Pulver und Schüttgüter, Springer-Verlag Heidelberg, ISBN 978-3-540-88448-4, (2009).

[Wes30] A.E. R. Westman, H.R. Hugill, The packing of particles, J. Am. Ceram. Soc.13, 10, 767-779, (1930).